Published in final edited form as:
J Autoimmun. 2011 December ; 37(4): 328–341. doi:10.1016/j.jaut.2011.09.005.

Tolerogen-induced interferon-producing killer dendritic cells (IKDCs) protect against EAE

Eduardo Huarte[1], **Agnieszka Rynda-Apple**[1], **Carol Riccardi**[1], **Jerod A. Skyberg**[1], **Sarah Golden**[1], **MaryClare F. Rollins**[1], **Andrew Ramstead**[1], **Larissa O. Jackiw**[1], **Massimo Maddaloni**[1], and **David W. Pascual**[1,2]

[1]Department of Immunology and Infectious Diseases, Montana State University, 960 Technology Blvd., Bozeman, Montana 59718, USA

Abstract

Natural killer (NK) cells and dendritic cells (DCs) have been shown to link the innate and adaptive immune systems. Likewise, a new innate cell subset, interferon-producing killer DCs (IKDCs), shares phenotypic and functional characteristics with both DCs and NK cells. Here, we show IKDCs play an essential role in the resolution of experimental autoimmune encephalomyelitis (EAE) upon treatment with the tolerizing agent, myelin oligodendrocyte glycoprotein (MOG), genetically fused to reovirus protein σ1 (termed MOG-pσ1). Activated IKDCs were recruited subsequent MOG-pσ1 treatment of EAE, and disease resolution was abated upon NK1.1 cell depletion. These IKDCs were able to kill activated $CD4^+$ T cells and mature dendritic DCs, thus, contributing to EAE remission. In addition, IKDCs were responsible for MOG-pσ1-mediated MOG-specific regulatory T cell recruitment to the CNS. The IKDCs induced by MOG-pσ1 expressed elevated levels of HVEM for interactions with cognate ligand-positive cells: $LIGHT^+$ NK and T_{eff} cells and $BTLA^+$ B cells. Further characterization revealed these activated IKDCs being MHC class II^{high}, and upon their adoptive transfer ($CD11c^+NK1.1^+$MHC class II^{high}), IKDCs, but not $CD11c^+NK1.1^+$MHC class $II^{intermediate/low}$ (unactivated) cells, conferred protection against EAE. These activated IKDCs showed enhanced CD107a, PD-L1, and granzyme B expression and could present OVA, unlike unactivated IKDCs. Thus, these results demonstrate the interventional potency induced $HVEM^+$ IKDCs to resolve autoimmune disease.

Keywords

EAE; tolerance; T_{reg} cells; IKDC; HVEM

[2]Corresponding author: David W. Pascual, Ph.D., Dept. of Immunology and Infectious Diseases, Montana State University, P.O. Box 173610, Bozeman, MT 59717-3610, USA. Phone: (406) 994-6244; Fax: (406) 994-4303; dpascual@montana.edu.

Conflict of interest
The authors have no financial conflict of interest.

Authorship contribution
E.H. and D.W.P. conceptualized and designed the experiments, analyzed the data, and prepared the manuscript; E.H., A.R-A., C.R., J.S., and M-C. R. performed the experiments and provided intellectual contributions; S.G., A.R-A., A.R., and M.M. designed and constructed the protein constructs; L. O. J. performed the cell-sorting experiments.

1. Introduction

The maintenance of immunological self-tolerance is an active process, requiring the participation of both the adaptive and innate immune systems. However, most efforts in studying tolerance have focused on the adaptive rather than on the innate arm of immunity; consequently, the innate immune system's contribution to tolerance is not as well understood, particularly the role of NK cells on autoimmunity [1, 2]. This regulatory role is suggested by NK cells' ability to recognize and efficiently lyse activated T cells [3], as well as act as a source of proinflammatory cytokines (IFN-γ, GM-CSF, and TNF-α) and chemokines (CCL3, CCL4, and CCL5) [4]. Previous studies suggest the existence of a cell subset, termed bitypic NK/DCs [5] or NKDCs [6], that shares phenotypical and functional features of both NK cells and DCs, despite the lack of an unambiguous set of phenotypic markers or a defined transcription factor. More recently, a new cell subset, referred to as interferon-producing killer dendritic cells (IKDCs) [7, 8], has been defined that shares features of both NK and DCs. Phenotypically, IKDCs have been originally described as $CD3^{-}$, $CD19^{-}$, $NK1.1^{+}$, $CD49b^{+}$, $CD11c^{intermediate}$, $B220^{+}$, $Gr\text{-}1^{-}$, and MHC class $II^{intermediate/high}$ [7, 8].

Functionally, IKDCs exhibit both cytolytic activity and MHC class II Ag presentation and therefore have been postulated as a bridge between the adaptive and innate arms of the immune system [7, 8]. It is still controversial whether IKDCs represent a separate lineage of DCs or merely a state of activation of NK cells, because poor Ag presentation capabilities by IKDCs is the heart of this debate. On one hand, IKDCs are able to present peptides to lymphocytes, but fail to process and present Ag to induce $CD4^{+}$ T cell proliferation [7, 9], suggesting IKDCs are activated NK cells. This point of view is accepted by several groups [10–12] and supported by data showing human NK cells having limited Ag presentation capacity once activated [13]. On the other hand, IKDCs may originate from different lymphoid precursors [14] and can become bona fide Ag-presenting cells after encountering virus [15] or tumor cells [16, 17], thus, supporting the notion of IKDCs as an independent cell lineage that truly shares phenotypic and functional features of NK cells and DCs.

Despite the recent focus on IKDCs' involvement in cancer [8, 15, 16] or viral infections [14], little or no information is available on the role IKDCs play in inflammatory diseases. Here, we show for the first time, to our knowledge, that IKDCs contribute to the resolution of EAE. Stimulation of IKDCs is noted after mucosal administration of an auto-Ag, myelin oligodendrocyte glycoprotein, fused to reovirus type 3 protein sigma 1 (termed MOG-pσ1). EAE is a T cell-dependent inflammatory disease principally mediated by IL-17 and is highly reproducible in susceptible rodent strains after immunization with TCR-reactive peptides and mimics some aspects of human multiple sclerosis (MS) [18]. Past efforts to induce modulation of autoimmunity by delivering auto-Ags have proven successful [19]; however, such efforts are hampered by requiring large doses of Ag or repeated administration. To overcome these barriers, we have found single dose tolerance or immunotherapy can be accomplished by genetically fusing Ags [20] or auto-Ags [21, 22] to (pσ1). Mucosal pσ1-delivered tolerogens have been found to induce IL-10-producing conventional regulatory T (T_{reg}) cells, as well as IL-4-producing Th2 cells, and when either subset is adoptively transferred, EAE could be reduced in an Ag-dependent fashion. Immunotherapy with MOG-pσ1 requires MOG to be coupled to pσ1, since pσ1 alone, pσ1 plus rMOG, or rMOG alone is unable to reverse EAE. Most notably, MOG-pσ1 could reverse EAE clinical disease within 24 h of treatment [22].

Although enhanced numbers of T_{reg} cells have been found to infiltrate the CNS after MOG-pσ1 treatment, understanding how this is accomplished within such a short time frame suggests possible innate cell involvement. In this context, the role of NK cells in the

development of EAE has received considerable attention in recent years. $NK1.1^+$ cells have been shown to be protective during the course of EAE [23,24], since depletion of NK cells with an anti-NK1.1 mAb leads to EAE exacerbation [25,26], which could be due to their cytotoxic effects upon activated autoreactive $CD4^+$ T cells or DCs [3]. Consequently, an enrichment of NK cells in the CNS of diseased animals leads to amelioration of EAE [26], while blocking the NK cell migration to the CNS exacerbates EAE [27, 28]. A protective effect of NK cells could also be attributed to the production of neuroprotective factors, such as the brain-derived neurotropic factor (BDNF) and neurotropin 3 (NT-3) [29]. Additionally, NK cell-produced IL-5 seems to play a protective role in MS [30], and MS patients present lower levels of NK cells [31], thus, suggesting a regulatory role for human NK cells. However, a consensus has yet to be reached over NK cells' role in the pathogenesis and development of EAE [32,33], since other groups have reported EAE amelioration after NK cell depletion [34] Interestingly, an immunoregulatory subset of human NK cells based on their expression of CD56 and IL-2Rαβγ levels has been proposed [35]. Supporting this hypothesis, the reduction of the clinical MS relapse rate during pregnancy is associated with an increase in the $CD56^{bright}$ (regulatory) subpopulation [36]. However, a similar phenotype is still lacking in murine models [33], and thus further studies are warranted in order to clarify the role of NK cells' involvement in EAE and other autoimmune diseases.

Herein we show IKDCs play a central role in the resolution of EAE following oral administration of MOG-pσ1. MOG-pσ1 induced an increase in the number of $CD11c^+NK1.1^+$ cells, but not conventional NK cells, in the periphery, as well as in the CNS of mice with EAE. $CD11c^+NK1.1^+$ cells were also able to lyse both DCs and activated $CD4^+$ T cells and, after MOG-pσ1 treatment, induced a robust proliferation by transgenic OVA TCR $CD4^+$ T cells, thus, fulfilling the definition of IKDCs and effectively providing a link between the adaptive and innate immune systems. Moreover, IKDCS from MOG-pσ1-treated mice showed a more activated phenotype than those from untreated controls, with an increase in the expression level of herpesvirus entry mediator (HVEM) and reduced expression of the inhibitory molecule NKG2A, allowing the lysis of $CD4^+$ T cells [37]. Interestingly, $NKG2A^+$ IKDCs were responsible for producing IL-10, a cytokine shown to have a pivotal role in the amelioration of EAE after MOG-pσ1 treatment [22]. In the absence of $NK1.1^+$ cells, MOG-pσ1 treatment failed to recruit T_{reg} cells into the CNS of diseased mice with a consequential loss of clinical efficacy. In addition, IKDCs were involved in the recruitment of activated ($CD69^+$) MOG-specific T_{reg} cells into the CNS. Importantly, MOG-pσ1 treatment also upregulated the level of expression of MHC class II molecules by CNS-infiltrating IKDCs. These MHC class II^{Hi} IKDCs presented a more activated phenotype than their MHC class $II^{intermediate/low}$ counterparts and showed enhanced expression of CD80, HVEM, granzyme B, CD107a (lysosomal associated membrane protein-1, LAMP-1) [38], and PD-L1 (programmed cell death 1 ligand, B7-H1) [39,40]. Adoptive transfer of these activated MHC class II^{Hi} IKDCs, but not $CD11c^+NK1.1^+$MHC $class^{intermediate/low}$ cells, dramatically improved the clinical resolution of EAE, underscoring the critical role played by IKDCs in treating EAE.

2. Materials and methods

2.1. Preparation of pσ1, MOG-pσ1, and MOG/GFP-pσ1

MOG-pσ1 and pσ1 were prepared, as previously described [22]. To enable detection of MOG-pσ1 binding, MOG-pσ1 was genetically modified to incorporate GFP. Briefly, MOG was removed with EcoRI from the MOG-pσ1 plasmid, and the remnant backbone was treated with calf intestine phosphatase and filled with a new EcoRI-SalI MOG and a SalI-EcoRI GFP fragments via a tripartite ligation. Recombinant clones were analyzed by DNA sequencing. The final construct for MOG/GFP-pσ1 was transformed into *Pichia pastoris* via electroporation (ECM630 BTX Harvard apparatus). Protein expression in yeast and protein

purification were performed, as previously described [22]. Proteins were assessed for purity and quality by Coomassie-stained polyacrylamide gels and by Western blot analysis, using an anti-His-tag mAb (Invitrogen, Carlsbad, CA).

2.2. Mice

Female 6–8 wk old C57BL/6 mice (Frederick Cancer Research Facility, National Cancer Institute, Frederick, MD) were used throughout the study. Breeding colonies of transgenic FoxP3-GFP, IL10$^{-/-}$, and OT-II mice (The Jackson Laboratory, Bar Harbor, ME) were maintained at Montana State University Animal Resources Center under pathogen-free conditions in individual ventilated cages under HEPA-filtered barrier conditions and were fed sterile food and water *ad libitum*. All animal care and procedures were in compliance with institutional policies for animal health and well-being.

2.3. EAE induction and MOG-pσ1-based therapies

For EAE induction, mice were challenged s.c. in the flank with 200 μg of $MOG_{35–55}$ peptide (Biosynthesis, Inc., Lewisville, TX) in 100 μl of IFA (Sigma-Aldrich, St. Louis, MO) containing 400 μg killed *Mycobacterium tuberculosis* (Difco Laboratories, Detroit, MI) on day 0. On days 0 and 2, mice were treated i.p. with 200 ng of *Bordetella pertussis* toxin (List Biological Laboratories, Campbell, CA). Mice were monitored and scored daily for disease progression: 0, normal; 1, a limp tail; 2, hind limb weakness; 3, hind limb paresis; 4, quadriplegia; 5, moribund state. When indicated, mice were given a single oral 50 μg dose of MOG-pσ1.

2.4. In vivo NK cell depletion

Mice were i.v injected with 500 μg/ml of anti-NK1.1 mAb (PK136; Bio X Cell, West Lebanon, NH) at the time of or 7 days after EAE challenge. Mice were subsequently treated weekly i.p. until day 21 p.ch.

2.5. Isolation of mononuclear cells from CNS

Mice were perfused through the left cardiac ventricle with cold PBS. The forebrain and cerebellum were dissected, and the spinal cords (SCs) flushed out with PBS by hydrostatic pressure and digested with 10 ml HBSS containing 500 U/ml of collagenase (Sigma-Aldrich) for 60–90 min at 37°C with shaking. The tissues were then homogenized in cold HBSS buffer (Sigma-Aldrich) with the plunger of a syringe, filtered through a 70 μm cell strainer to obtain a single cell suspension, and centrifuged. Cell pellets from 4–5 mice were pooled, resuspended in 70% Percoll (Sigma-Aldrich), and underlaid with 30% Percoll. Mononuclear cells were isolated from the 30/70 interphase after gradient density centrifugation, washed, and stained for flow cytometry.

2.6. Tetramer staining

Tetramer-based enrichment was performed similar to that previously described [41]. Briefly, CNS-infiltrating lymphocytes and splenocytes were first stained with $MOG_{42–55}$ -APC or $OVA_{329–337}$-APC tetramer (NIH Tetramer Core Facility, Emory Univ., Atlanta, GA) for 1h at room temperature in PBS containing 2% of FBS, 2% rat serum, and Fc block (BD Pharmingen). Cells were then stained with anti-APC magnetic beads (Miltenyi Biotec, Bergisch Gladbach, Germany) following the manufacturer instructions and then passed over a magnetized column (Miltenyi Biotec) to separate bound and unbound fractions. The resulting fractions were then stained for extracellular markers and acquired fluorescence using a LSR-II flow cytometer (Becton Dickinson, San Jose, CA) and analyzed with Flow Jo software (Tree Star Inc., Ashland, OR).

2.7. Cytokine ELISAs

Spleens were removed 18 – 21 days after EAE induction from PBS and MOG-pσ1 treated mice. Bead-isolated $CD25^+CD4^+$ or $CD25^-CD4^+$ T cells (>95% purity) were cultured for 4 days in the presence of 1:1 ratio of T cell-depleted splenic feeder cells with or without $MOG_{35–55}$ restimulation. Capture ELISA was employed to quantify the levels of IFN-γ, IL-10, IL-17, and TGF-β, as previously described [22].

2.8. Characterization and isolation of IKDCs

Splenic and lymph node (LN) cells including mesenteric LNs (MLNs) and head and neck LNs (HNLNs) were stained with biotinylated or fluorochrome-conjugated mAbs against B220 (clone RA3-6B2), CD1d (1B1), CD3 (145-2C11), CD25 (PC61), CD5 (53-7.3), CD11c (HL3), and CD49b (Ha1/29), all from BD Pharmingen. CD4 (GK1.5), CD107a (1D4B), NKG2D (clone C7), and TRAIL (N2B2) mAbs were obtained from Biolegend (San Diego, CA). NK1.1 (PK136), NKG2A (16A11), HVEM (LH1), BTLA (8F4), MHC-II (M5/114.15.2), and CD11b (M1/70) mAbs were obtained from eBioscience; anti-PD-L1 mAb was from Serotec; and anti-LIGHT mAb was from R & D Systems. Intracellular staining for FoxP3, IFN-γ, granzyme B, and IL-10 was accomplished using FITC-, PE-Cy5-, or PE-labeled mAbs (eBioscience), and PE- or APC-anti-IFN-γ or -anti IL-10 mAbs (BD Pharmingen). Cells were acquired using a LSR-II flow cytometer (Becton Dickinson) and analyzed with Flow Jo software (Tree Star Inc.). Cell-sorting was accomplished using a FACSAria (Becton Dickinson), as previously described [16]. Briefly, spleens and LNs were stained for CD3, CD11c, B220, MHC class II, CD11b, and NK1.1, and three different populations were sorted based on the expression of CD11c, NK1.1, and MHC class II. IKDCs were confirmed to be $B220^+$ and $CD3^-$. Cell purity exceeded 95%.

2.9. MOG/GFP-pσ1 binding assays

Splenic cells from naïve or EAE mice were incubated at 4°C with 20 μg/ml of MOG/GFP-pσ1 for 30 min, washed, and stained with mAbs to NK1.1 (clone PK136, eBioscience); CD11c (HL3, BD Pharmingen); B220 (RA3-6B2, BD Pharmingen); and HVEM (LH1, eBioscience) for another 20 min before being analyzed by flow cytometry.

2.10. Adoptive transfer

C57BL/6 mice were challenged with $MOG_{35–55}$, as described above, and 15 days later, they were orally treated with 50 μg of MOG-pσ1. Twenty-four h later, spleens and LNs were combined and sorted, as indicated above. $1×10^5$ $CD11c^+NK1.1^+$ MHC class II^{high} IKDCs or $CD11c^+NK1.1^+$ MHC class II^{low} cells were adoptively transferred i.v. into C57BL/6 mice already $MOG_{35–55}$-challenged 7 days earlier.

2.11. Proliferation assay

Briefly, $1 × 10^5$ purified OT-II $CD4^+$ T cells were stimulated with $OVA_{323–339}$ (2.0 μg/ml) or OVA (1 mg/ml) in the presence of irradiated (3000 rad) NK cells, DCs, or IKDCs as a source of Ag-presenting cells for 4 days. When indicated, Ag-presenting cells were pretreated with B16F1 melanoma cells (ATCC, Manassas, VA) at a ratio of 10:1 or 10 μg/ml of MOG-pσ1 for 30 min at 4°C. One μCi per well of [^{3}H]-thymidine was added during the last 12 h of incubation. The cells were then harvested, and incorporated [^{3}H]-thymidine was counted using a Beckman LS 6500 scintillation counter.

2.12. ^{51}Chromium release assay

Cytotoxic assays were performed using DCs, $CD4^+$ T cells, or YAC-1 lymphoma cells (ATCC) as target cells. Briefly, 1 H 10^6 target cells were incubated with 50 μCi of ^{51}Cr for 2 h at 37°C. Labeled cells were washed three times and then incubated with varying

numbers of effector cells. For concanamycin A (CMA; Wako Bioproducts, Richmond, VA) treatment, 100 nM of CMA was added to desired wells. After 4 h incubation, 100 μl of each supernatant was harvested and radioactivity counted using a Beckman LS 6500 scintillation counter. Specific lysis was calculated by measuring the level of released ^{51}Cr from target cells corrected for spontaneous release/total ^{51}Cr release obtained by detergent (5% Triton X-100) lysis × 100. Spontaneous lysis was measured from wells containing only labeled target cell [42].

2.13. Statistical analysis

The ANOVA followed by posthoc Tukey test was applied to show differences in clinical scores in treated versus PBS mice. The student t test was used to evaluate the differences between percentages of positive cells between groups, and *P*-values < 0.05 are indicated.

3. Results

3.1. MOG-pσ1 abates EAE, and this therapeutic effect is abrogated upon NK1.1 mAb depletion

Mucosal application of the fusion protein, MOG-pσ1, is effective against EAE in both prophylactic and therapeutic regimens. In fact, a single oral dose at the peak of disease resulted in significant 3-fold reduction in clinical scores within 24 h after treatment (Fig. 1A). This resolution in EAE was accompanied by 3-fold increase in the number of $NK1.1^+$ cells in the spleens of treated mice (Fig. 1B). To investigate further if MOG-pσ1's protective effect was mediated by $NK1.1^+$ cells, mice were treated with a depleting PK136 mAb [24], starting at 0 or 7 days after EAE induction (Fig. 1C). Mice continued to receive weekly PK136 mAb treatments until day 21 p.ch, and $NK1.1^+$ cell depletion significantly augmented EAE for either treatment. Furthermore, MOG-pσ1's protective effect was abated in mice depleted of their $NK1.1^+$ cells (Fig. 1D). These data confirmed previous reports that highlighted the relevance of NK cells for EAE clearance [25, 26] and indicated MOG-pσ1's clinical benefits were, at least partially, dependent on $NK1.1^+$ cells.

3.2. NK1.1 cell depletion abrogates MOG-pσ1-mediated recruitment of FoxP3$^+$ T_{reg} cells

Confirming our previous finding that MOG-pσ1 treatment induced an up-regulation in the number of $FoxP3^+$ T_{reg} cells in the spleens of treated mice (Fig. 1E and F; [22]), we questioned whether this increase was NK cell-dependent. Mice with EAE were NK1.1 mAb-depleted at the peak of disease (day 18) and, on day 20, were treated with MOG-pσ1 or PBS. Mice previously treated with the depleting mAb showed a reduced number of $FoxP3^+$ $CD25^+CD4^+$ T cells in their LNs (Fig. 1G), while there was no effect on the number of T_{reg} cells on the spleens (Supplementary Fig. S1). Moreover, CNS-infiltrating BM-derived cells showed a significantly lower percentage of $FoxP3^+$ T_{reg} cells in GFP-FoxP3 reporter mice depleted of NK1.1 cells when compared with PBS-treated mice (Fig. 1H), further implicating the significance for $NK1.1^+$ cells or their subsets in T_{reg} cell recruitment.

3.3. Induced T_{reg} cells are MOG-specific

Since conventional staining for MOG class II tetramers fails to detect low avidity Ag-specific $CD4^+$ T cells [43], a cell enrichment step [41] was performed to enable detection of MOG-specific T_{reg} cells. Splenocytes from EAE mice (day 15 p.ch, score 1–2) were stained with $OVA_{329–337}$ or $MOG_{42–55}$ tetramers prior to magnetic purification, and only the (column) bound fraction was stained with $MOG_{42–55}$ tetramer (Fig. 2A). Subsequent analysis of splenocytes and CNS-infiltrating lymphocytes from severely sick (day 18, score 3–4) FoxP3-GFP reporter mice, the majority of CNS-infiltrating $FoxP3^+$ $CD4^+$ T cells in the bound fraction were tetramer-specific (Fig 2B-C), as opposed to $CD8^+$ T cells (data not

shown). Thus, MOG-pσ1 treatment enhanced the absolute number of tetramer-specific CNS-infiltrating T_{reg} cells (Fig. 2C). Moreover, most of the FoxP3$^+$ tetramer-specific SC-infiltrating lymphocytes appeared activated since these were CD69$^+$ (Fig. 2D), unlike naive tetramer-negative CD25$^+$CD4$^+$ T cells (Fig. 2D). Thus, this analysis demonstrates MOG-pσ1 treatment enhances the recruitment of MOG-specific T_{reg} cells into the CNS.

To determine the responsible cytokines induced by MOG-pσ1, cytokine analyses were performed on purified splenic CD25$^-$CD4$^+$ and CD25$^+$CD4$^+$ T cells isolated at the peak of the clinical EAE (around day 20 p.ch) from mice treated with MOG-pσ1 or PBS 24h earlier. T_{reg} cells from MOG-pσ1-treated mice showed significant elevations in IL-10 when compared to T_{reg} cells from diseased PBS-treated mice ($p < 0.01$) with concomitant reductions in IFN-γ and IL-17 ($p < 0.01$; Fig. 2E). There were no significant changes in TGF-β production (Fig. 2E). These results show MOG-pσ1-stimulated T_{reg} cells protect via IL-10 with concomitant inhibition of IL-17and IFN-γ in a MOG-specific fashion.

3.4. MOG-pσ1 increases the number of CD11c$^+$NK1.1$^+$ cells

Further analysis of the NK cell phenotype revealed that MOG-pσ1 treatment of EAE mice enhanced the numbers of CD11c$^+$NK1.1$^+$ cells, but not conventional CD11c$^-$NK1.1$^+$ NK cells, in their spleens relative to PBS-treated mice (Fig. 3A). This population of cells expressed high levels of surface B220, MHC class II, and CD49b (Fig. 3A), as others have found [7, 8]. Stimulation with $MOG_{35–55}$ showed these cells were IFN-γ$^+$ (Fig. 3A), again, in concordance with these original studies. Given that MOG-pσ1 treatment enhanced CD11c$^+$NK1.1$^+$ cells in diseased mice, we queried if MOG-pσ1 treatment in the absence of EAE could induce CD11c$^+$NK1.1$^+$ cells in naïve mice. While naïve mice showed almost no CD11c$^+$NK1.1$^+$ cells, oral MOG-pσ1 treatment augmented the presence of these cells in spleens and MLNs (Fig. 3B). However, this increase in CD11c$^+$NK1.1$^+$ cells was transient, and mice challenged with EAE 40 days earlier showed no increased numbers of this subset. Interestingly, EAE mice treated with MOG-pσ1 had negligible amount of CD11c$^+$NK1.1$^+$ cells in the MLNs (Fig. 3B), while ~1.0% of CD45^{Hi} CD11b$^+$ BM-derived cells infiltrating the CNS were CD11c$^+$NK1.1$^+$ cells versus ~0.3% found in the PBS-treated EAE mice (Fig. 3C). A modest increase in the percentage of CD11c$^+$NK1.1$^+$ in the bone marrow of EAE versus naive mice ($p < 0.05$) was also found, although MOG-pσ1 intervention failed to further increase this percentage (Supplementary Fig. S2).

3.5. CD11c$^+$NK1.1$^+$ cells are phenotypically compatible with IKDCs and produce IL-10

To determine if the CD11c$^+$NK1.1$^+$ cells were indeed IKDCs, a more detailed phenotypic and functional analysis was performed. CD11c$^+$NK1.1$^+$ cells expressed elevated levels of both CD80 and CD86 in spleens (Fig. 4A, left panels) and MLNs (Fig. 4A, right panels). Strikingly, although SC-infiltrating CD11c$^+$NK1.1$^+$ cells were MHC class II$^{intermediate/low}$, MOG-pσ1 treatment induced a dramatic up-regulation of MHC class II (Fig. 4B). Both conventional CD11c$^-$ NK1.1$^+$ NK cells and CD11c$^+$NK1.1$^+$ cells co-expressed the NK cell markers, NKG2D, NKG2A, and TRAIL (Fig. 4C and data not shown), while CD11c$^+$NK1.1$^-$ DCs were negative for these NK molecules (Fig. 4C). Although MOG-pσ1 treatment appeared to have no effect on the expression of the stimulatory molecule, NKG2D, CNS-infiltrating CD11c$^+$NK1.1$^+$ cells in MOG-pσ1-treated mice showed reduced expression of the inhibitory molecule, NKG2A (Fig. 4D). However, since MOG-pσ1 treated animals showed increased numbers of SC-infiltrating IKDCs, the total number of NKG2A$^+$ IKDCs was greater in MOG-pσ1-treated than PBS-treated mice (Fig. 4D). Interestingly, while DCs and conventional CD11c$^-$ NK1.1$^+$ cells did not produce IL-10, approximately 50% of CD11c$^+$NK1.1$^+$ cells produced IL-10 two weeks after EAE induction (Fig. 4E). After MOG-pσ1 treatment, IL-10 production by NK1.1$^+$ cells was restricted to the NKG2A$^+$ subset (Fig. 4F).

3.6. CD11c$^+$NK1.1$^+$ cells are functionally compatible with IKDCs and can present peptide Ags

To determine if the CD11c$^+$NK1.1$^+$ cells were functionally compatible with the definition for IKDCs, their cytolytic activity and Ag presentation capacities were analyzed. In addition to lysing NK cells' targets, YAC-1 cells, the CD11c$^+$NK1.1$^+$ cells effectively lysed activated CD4$^+$ T cells and mature DCs (Fig. 5A). Supporting this notion for IKDCs, their cytolytic activity was inhibited by > 50% in the presence of concanamycin A (CMA), indicating their mechanism of killing is perforin-dependent [44] (Fig. 5B).

To assess their capacity as Ag-presenting cells, CD11c$^+$NK1.1$^-$ DCs, CD11c$^-$NK1.1$^+$ NK cells, or CD11c$^+$NK1.1$^+$ cells were isolated from naive mice, mice just starting to show clinical symptoms of EAE (day 12, score 1), or from severely sick mice (day 21, score 3). Subsequently, the individual subsets were pulsed with OVA or $OVA_{323–339}$ to activate OT-II CD4$^+$ T cells. Although CD11c$^+$NK1.1$^+$ cells were able to present $OVA_{323–339}$ peptide, they failed to induce strong OT-II cell proliferation when pulsed with intact OVA (Fig. 5C), unlike conventional DCs. However, the previously observed up-regulation of MHC class II molecules after MOG-pσ1 treatment (Fig. 4B) prompted us to investigate whether MOG-pσ1 treatment had any effect on their ability to process and present Ag. Indeed, when the CD11c$^+$NK1.1$^+$ cells were incubated with OVA protein in the presence of MOG-pσ1, they were able to stimulate the proliferation of OT-II CD4$^+$ T cells (Fig. 5D), albeit not as efficiently as conventional DCs isolated from the same mice, thus, fulfilling their functional definition as Ag-presenting cells. Similarly, treatment of CD11c$^+$NK1.1$^+$ cells with B16F1 melanoma cells prior to OVA incubation also enhanced specific CD4$^+$ T cell proliferation, consistent with that previously reported [17]. Thus, the observed CD11c$^+$NK1.1$^+$ subset truly shares both phenotypical and functional characteristics of NK cells and DCs and consequently is considered IKDCs.

3.7. MOG-pσ1 treatment up-regulates HVEM expression by NK1.1$^+$ cells

Since IKDCs were enhanced in the spleen and CNS following MOG-pσ1 treatment of EAE mice, we queried if MOG-pσ1 treatment had any impact upon the number of CNS-infiltrating IKDCs. Interestingly, while a significant proportion of NK1.1$^+$ cells were positive for the co-stimulatory molecule HVEM, CD4$^+$ T cells were mostly positive for the HVEM ligand, LIGHT [48,49] (Fig. 6A), while B220$^+$ B cells were positive for the co-inhibitory molecule BTLA (B and T lymphocyte attenuator; data not shown), another HVEM ligand [45]. Interestingly, B220$^+$CD5$^+$ regulatory B cells, but not B220$^+$CD5$^-$ inflammatory B cells [46], were also LIGHT$^+$ (Fig. 6B). Furthermore, a significant increase was found in the number of HVEM$^+$ IKDCs (both in the SCs and spleens) of MOG-pσ1-treated mice (Fig. 6C and D). A kinetic analysis of HVEM expression of splenic IKDCs following EAE induction showed a rapid up-regulation of HVEM, peaking around day 14. Such up-regulation of HVEM levels was not evident in IL-10$^{-/-}$ mice, although these mice showed aggravated disease (average maximum score 4.5 versus 2.5 in wt mice (data not shown), further suggesting the relevance of HVEM$^+$ NK1.1$^+$ cells in the resolution of EAE (Fig. 6D). Overall, these data suggest an important role for HVEM expression by IKDCs, either directly acting as an activator of IKDCs or indirectly as an inhibitor of BTLA/LIGHT$^+$ CD4$^+$ T or B cells. Consequently, the observed up-regulation of HVEM by IKDCs after MOG-pσ1 treatment may provide a rationale for the observed clinical improvement.

3.8. HVEM$^+$ IKDCs bind MOG-pσ1

To assess whether MOG-pσ1 directly interacts with IKDCs, we took advantage of a MOG/GFP-pσ1 construct to perform a cell binding study. Splenocytes from naïve mice, mice with EAE (day 21, score 2–2.5), or mice recovering from EAE (day 40, score 1) were incubated with MOG/GFP-pσ1 or PBS. Interestingly, only HVEM$^+$ NK1.1$^+$ cells were able to bind

MOG/GFP-pσ1 protein. Consequently, NK1.1$^+$ cells derived from day 21 EAE mice showed the greatest binding (61.5 ∀ 5.2 of total NK1.1$^+$ cells vs. 6.3 ∀ 1.8 in the naïve group) (Fig. 7A and B). To assess whether MOG-pσ1 binding to HVEM$^+$ NK1.1$^+$ cells was mediated via MOG or pσ1, binding assays were performed in the presence of an anti-HVEM mAb (20 μg/ml), recombinant MOG, or increasing concentrations of recombinant pσ1 (20 and 100 μg/ml). Only pσ1 was able to significantly reduce the binding of MOG-pσ1 to the HVEM$^+$ NK1.1$^+$ cells (Fig. 7B), showing that, although HVEM is an activation marker on NK cells, it does not directly bind to MOG-pσ1. A GFP-pσ1 construct (lacking MOG) was also able to effectively bind to HVEM$^+$ NK1.1$^+$ cells, further confirming pσ1 responsible for the binding (data not shown).

Further analysis of the subpopulation bound to MOG/GFP-pσ1 showed that CD11c$^+$ NK1.1$^+$ IKDCs, but not CD11c$^+$NK1.1$^-$ DCs or CD11c$^-$NK1.1$^+$ NK cells, were able to bind MOG/GFP-pσ1 protein (Fig. 7C). Again, MOG-pσ1 binding was restricted to the HVEM$^+$ subpopulation (Fig. 7C), further suggesting the importance of the HVEM$^+$ IKDC population in the MOG-pσ1 associated clinical resolution of EAE.

3.9. Adoptive transfer of IKDCs protects against EAE

To further investigate the role of IKDCs in EAE, a FACS-sorting strategy was optimized to allow isolation of IKDCs from NK cells and DCs from MOG-challenged mice (day 15 p.ch). CD11c$^+$NK1.1$^+$ IKDCs were further subdivided into MHC class II^{Hi} IKDCs or MHC class II$^{intermediate/low}$ cells (Fig. 8A) [15,33]. As previously reported [17], about a third of the CD11c$^+$NK1.1$^+$MHC class II^{Hi} subset was also CD11b$^+$ in contrast to the CD11b$^-$ CD11c$^+$ NK1.1$^+$MHC class II$^{intermediate/low}$ cells (Fig. 8B). Interestingly, the MHC class II^{Hi} subset also expressed higher levels of CD80 than their MHC class II$^{intermediate/low}$ counterparts (Fig. 8B). As expected, the vast majority of DCs was MHC class II^{high}, while CD11c$^-$NK1.1$^+$ (NK) cells were MHC class II-negative (Fig. 8C). When FACS-sorted activated MHC class II^{high} IKDCs versus unactivated IKDCs and were adoptively transferred into mice challenged with $MOG_{35–55}$ 7 days earlier, only MHC class II^{Hi} IKDCs were able to significantly reduce EAE (Fig. 8D). Interestingly, mice adoptively transferred with unactivated IKDCs showed slightly more severe disease than the PBS control group during the first 20 days of the disease, and in fact they failed to resolve EAE (Fig. 8D). These data demonstrate MHC class II^{Hi} IKDCs, not MHC class II$^{intermediate/low}$ cells, are essential for dampening EAE, providing a clinical benefit mediated by MOG-pσ1 intervention.

3.10. Activated IKDCs up-regulate HVEM, CD107a, PDL-1, and granzyme B and act as Ag-presenting cells

Since MOG-pσ1 exclusively bound to HVEM$^+$ IKDCs (Fig. 7), we queried whether MHC class II^{Hi} IKDCs overexpressed HVEM. Indeed, MHC class II^{Hi} IKDCs showed significantly higher levels of HVEM when compared to MHC class II$^{intermediate/low}$ cells (Fig. 9A), thus, providing a rationale for MOG-pσ1's therapeutic effects. When IKDCs and NK cells were cultured with the NK target cell line YAC-1, a profound up-regulation in CD107a, PD-L1, and granzyme B, by the MHC class II^{Hi} IKDCs, not NK cells, further suggested a critical role for IKDCs in EAE recovery (Fig. 9B and C). Interestingly, both PD-L1 and CD107a levels were much higher for IKDCs than on NK cells (Fig. 9C). However, when IKDCs were cultured with YAC-1 cells in the presence of mAbs specific for either BTLA or HVEM, this up-regulation was abolished, again suggesting the protective role of IKDCs was mediated by this HVEM/BTLA interaction (Fig. 9C).

To assess whether activated MHC class II^{Hi} IKDCs were responsible for Ag presentation, as shown above (Fig. 4D), NK1.1$^+$ CD11c$^-$, NK1.1$^-$ CD11c$^+$, NK1.1$^+$ CD11c$^+$ MHC class

II^{Hi}, and $NK1.1^+$ $CD11c^+$ MHC class $II^{intermediate/low}$ cells were purified from EAE mice (day18 p.ch), and cells were pulsed with OVA overnight prior to being co-cultured with OT-II $CD4^+$ T cells. Only conventional DCs ($NK1.1^-$ $CD11c^+$) and activated IKDCs ($NK1.1^+$ $CD11c^+$ MHC II^{Hi}) were able to induce a strong proliferation of $CD4^+$ T cells (Fig. 9D), suggesting that only activated IKDCs ($NK1.1^+$ $CD11c^+$ MHC class II^{Hi}) show the effector function required for protection against EAE.

4. Discussion

MS is a neurodegenerative disease of the CNS that involves infiltration of activated inflammatory cells, damaging both myelin and axons, and is the most prevalent cause of paralysis in young adults [32]. EAE, a rodent model for MS, shares many of the same features [47] of this neurodegenerative disease and is T cell-mediated. Although MS has been studied for more than 150 years, an effective and safe therapy for MS remains elusive [48]. However, IFN-β1a treatment has proven to be therapeutic for MS, enhancing both the number and activity of T_{reg} cells and the percentage of $CD56^{bright}$ NK cells [32, 49], a subset associated with clinical remissions [50] and reduced brain MRI lesions [51, 52]. However, up to 50% of patients do not respond to type I IFNs [53]. Moreover, both EAE models and clinical trials have shown that IFN-β treatment reduces clinical symptoms in Th1 cell-driven disease, but worsens Th17 cell-induced disease by a mechanism that remains unclear [54,55]. Altogether, the available data indicate the relevance of IFNs in MS and possibly the importance of these described IKDCs, a source of IFNs. Other therapies, such as glatiramer acetate [56, 57] or mAbs, Rituximab [58], Daclizumab [59] and Alemtuzumab [60], directed against CD20, CD25, and CD52, respectively, are currently under clinical investigation and have promising efficacy, although some safety concerns remain [48].

IKDCs resemble both NK cells and DCs and were originally described as $CD11c^{int}$ $B220^+$ $NK1.1^+$ $CD3^-$ $CD19^-$ $Gr\text{-}1^-$ cells [7,8]. However, acceptance of this novel lymphoid subset as a specific entity has yet to be widely accepted, partially, because of its lack of a unique cell surface marker or a defined transcriptional factor. Consequently, reliance on shared phenotypic markers, as well as functional attributes, is required to characterize IKDCs. In this regard, IKDCs are found to exert potent anti-tumor activity through the secretion of IFN-γ and direct killing of tumor cells. Although some controversy remains over their Ag presentation capacity (and if consequently these truly constitute a separate lineage of DCs or a mere state of activation of NK cells), recent data [17] indicate that at least a subset of IKDCs (the $CD11b^+$ fraction) is licensed by tumor cells to acquire DC-like function by gaining the ability to process and present Ags to naive T cells. Consequently, it was found IKDCs could present OVA or $OVA_{323–339}$ to OT-II T cells, but, unlike conventional DCs, failed to stimulate strong proliferative $CD4^+$ T cell responses to intact OVA. However, MOG-pσ1 treatment enhanced MHC class II levels on IKDCs, suggesting such treatment may enhance their ability to present Ag. Since B16F1 melanoma cells can stimulate $CD11b^+$ IKDCs to process and present Ag [17], it was indeed found treatment of $CD11c^+NK1.1^+$ cells with either B16F1 or MOG-pσ1 significantly enhanced Ag presentation. This collective evidence shows that MOG-pσ1-induced IKDCs share both phenotypical and functional attributes of both DC and NK cells, suggesting these are truly IKDCs.

A marked increase in the number of $CD11c^+NK1.1^+$ cells in MOG-pσ1-treated EAE mice was observed. These IKDCs (predominately $B220^+$ $CD11b^+$ $CD49b^{+)}$ produced IFN-γ following $MOG_{35–55}$ restimulation, yet could also produce IL-10, a potent immunomodulatory cytokine. It has been previously reported that co-production of IFN-γ and IL-10 by NK cells dampens inflammatory responses [61], further implicating the relevance of these cells in EAE remission. In addition, $CD11c^+NK1.1^+$ cells were also able

to efficiently lyse YAC-1 cells, suggesting these are NK cells, and also, albeit with a lower avidity, lyse activated $CD4^+$ T cells and mature DCs, as previously reported [3]. While reduced expression of the NK cell inhibitory molecule, NKG2A, was observed after MOG-pσ1 treatment, the total number of $NKG2A^+$ IKDCs in the CNS was markedly enhanced, and IL-10 production was limited to these $NKG2A^+$ cells. Given these findings, it is possible that IKDC cytolytic and regulatory activities may contribute to resolving EAE.

Upon evaluating the activation status of IKDCs, a dramatic up-regulation of HVEM was found after EAE induction, and these cells showed enhanced MOG-pσ1 binding, suggesting a possible relationship between HVEM expression and the capacity of IKDCs to become responsive to MOG-pσ1 treatment. HVEM belongs to the tumor necrosis factor receptor family and regulates host immune responses to various pathogens and autoiummune diseases upon interactions with one of several ligands. Aside from binding herpesvirus gD protein, HVEM is able to bind Ig superfamily members, BTLA and CD160, and TNF superfamily ligands, LIGHT and LTα [45]. Of these, HVEM interactions with BTLA and LIGHT are of especial interest, since LIGHT is expressed by the majority of $CD4^+$ T cells and regulatory $B220^+CD5^+$ B cells [46] in our system, and virtually all of the B cells are positive for BTLA. Engagement of HVEM by *trans* interaction with BTLA or LIGHT has been reported to induce co-stimulatory signaling and promote cell survival via activation of NF-κB [62]and IFN-γ production and to increase anti-tumor activity of NK cells [63]. On the other hand, HVEM signaling through BTLA leads to inactivation mediated by SH2 domain-containing protein tyrosine phosphatases 1 and 2 [64]. Due to this dual capacity of delivering both costimulatory and inhibitory signals, HVEM is often considered a molecular switch of the immune system [45,65]. In our case, expression of HVEM by IKDCs may lead to inactivation of BTLA-expressing $CD4^+$ T lymphocytes, as well as IKDC activation through interaction with $LIGHT^+$ $CD4^+$ T cells or BTLA-expressing B cells. As previously suggested, *cis* interactions between double positive HVEM and BTLA IKDCs may also be occurring [rev. in 45]. A significant proportion of regulatory $B220^+CD5^+$ B cells are also positive for LIGHT and therefore may be implicated in the activation of $HVEM^+$ IKDCs. Additional studies are currently under way to further elucidate the complex role of HVEM/BTLA/LIGHT in EAE.

This work also shows T_{reg} cells play a critical role in the resolution of EAE following MOG-pσ1 treatment, thus, confirming our previous findings. Analysis of the CNS-infiltrating T_{reg} cells showed these to be MOG-specific following staining with MHC class II tetramers, and to be more activated evident by the increased numbers of $CD69^+$ T_{reg} cells present in the CNS in MOG-pσ1-treated mice than in EAE diseased mice. More importantly, this beneficial impact by MOG-pσ1 is dependent on $NK1.1^+$ cells, since mice treated with a depleting anti-NK1.1 mAb failed to recruit T_{reg} cells and resulted in no clinical improvement. One possible explanation for this finding is the loss of DCs via cytolysis by MOG-pσ1-activated IKDCs, since cross-talk between DCs and T_{reg} cells has been well-established [66]. IKDCs express high levels of NKG2A, which is consistent with this hypothesis [67]. Alternatively, there could be direct interaction between NK and T_{reg} cells through BTLA/HVEM ligation or NK cell-dependent CCL22 secretion [68]. Additional studies are warranted to determine how cells interact to resolve autoimmunity.

MHC class II levels in conjunction with NK1.1 and CD11c have previously been considered the only unambiguous marker for IKDCs [15,33]. Here we show MHC class II^{Hi} $CD11c^+NK1.1^+$ activated IKDCs, but not the unactivated MHC class $II^{intermediate/low}$ $CD11c^+NK1.1^+$ cells, are able to induce a strong $CD4^+$ T cell proliferation and, more importantly, prevent EAE development after adoptive transfer into MOG-challenged mice, further indicating the relevance of this population of cells in the development of autoimmune disorders. Since activated IKDCs up-regulate HVEM, they are an obvious

candidate to mediate MOG-pσ1's effects. Interestingly, IKDCs also up-regulate the effector molecules granzyme B, CD107a, and PD-L1. During the last few years, PD-1/PD-L1 interaction has emerged as a critical regulator of EAE and other autoimmune diseases [39,69]. The observed PD-L1 up-regulation may contribute to the clinical effect through the inhibition of PD-1^+ encephalitogenic $CD4^+$ T cells [69].

To the best of our knowledge, this is the first work in which IKDCs are demonstrated to be protective in autoimmune diseases, thus, opening the door to future clinical interventions. However, further studies are needed in order to unambiguously dissect all the multiple proposed mechanisms of action (IL-10 production, HVEM up-regulation, T_{reg} cell recruitment, cytolytic activity, PD-1 ligation, and Ag presentation) and their relative clinical relevance.

Supplementary Material

Refer to Web version on PubMed Central for supplementary material.

Acknowledgments

We thank the NIH Tetramer Core Facility for kindly providing us with MHC class II tetramers used in this study and Ms. Nancy Kommers for her assistance in preparing the manuscript. This work is supported by U.S. Public Health Service Grant R01 AI-078938 and, in part, by Montana Agricultural Station and U.S. Department of Agriculture Formula Funds. The Department of Immunology and Infectious Diseases' flow cytometry facility was, in part, supported by NIH/National Center for Research Resources, Centers of Biomedical Excellence P20 RR-020185, and an equipment grant from the M.J. Murdock Charitable Trust.

References

1. Flodstrom-Tullberg M, Bryceson YT, Shi FD, Hoglund P, Ljunggren HG. Natural killer cells in human autoimmunity. Curr Opin Immunol. 2009; 21:634–40. [PubMed: 19892538]
2. Paust S, Senman B, von Andrian UH. Adaptive immune responses mediated by natural killer cells. Immunol Rev. 2010; 235:286–96. [PubMed: 20536570]
3. Rabinovich BA, Shannon J, Su RC, Miller RG. Stress renders T cell blasts sensitive to killing by activated syngeneic NK cells. J Immunol. 2000; 165:2390–7. [PubMed: 10946262]
4. Marcenaro E, Della Chiesa M, Bellora F, Parolini S, Millo R, Moretta L, et al. IL-12 or IL-4 prime human NK cells to mediate functionally divergent interactions with dendritic cells or tumors. J Immunol. 2005; 174:3992–8. [PubMed: 15778356]
5. Homann D, Jahreis A, Wolfe T, Hughes A, Coon B, van Stipdonk MJ, et al. CD40L blockade prevents autoimmune diabetes by induction of bitypic NK/DC regulatory cells. Immunity. 2002; 16:403–15. [PubMed: 11911825]
6. Pillarisetty VG, Katz SC, Bleier JI, Shah AB, Dematteo RP. Natural killer dendritic cells have both antigen presenting and lytic function and in response to CpG produce IFN-γ via autocrine IL-12. J Immunol. 2005; 174:2612–8. [PubMed: 15728467]
7. Chan CW, Crafton E, Fan HN, Flook J, Yoshimura K, Skarica M, et al. Interferon-producing killer dendritic cells provide a link between innate and adaptive immunity. Nat Med. 2006; 12:207–13. [PubMed: 16444266]
8. Taieb J, Chaput N, Menard C, Apetoh L, Ullrich E, Bonmort M, et al. A novel dendritic cell subset involved in tumor immunosurveillance. Nat Med. 2006; 12:214–9. [PubMed: 16444265]
9. GeurtsvanKessel CH, Bergen IM, Muskens F, Boon L, Hoogsteden HC, Osterhaus AD, et al. Both conventional and interferon killer dendritic cells have antigen-presenting capacity during influenza virus infection. PLoS One. 2009; 4:e7187. [PubMed: 19784375]
10. Blasius AL, Barchet W, Cella M, Colonna M. Development and function of murine $B220^+CD11c^+NK1.1^+$ cells identify them as a subset of NK cells. J Exp Med. 2007; 204:2561–8. [PubMed: 17923504]

11. Caminschi I, Ahmet F, Heger K, Brady J, Nutt SL, Vremec D, et al. Putative IKDCs are functionally and developmentally similar to natural killer cells, but not to dendritic cells. J Exp Med. 2007; 204:2579–90. [PubMed: 17923506]
12. Vosshenrich CA, Lesjean-Pottier S, Hasan M, Richard-Le Goff O, Corcuff E, Mandelboim O, et al. $CD11c^{lo}B220^{+}$ interferon-producing killer dendritic cells are activated natural killer cells. J Exp Med. 2007; 204:2569–78. [PubMed: 17923507]
13. Hanna J, Gonen-Gross T, Fitchett J, Rowe T, Daniels M, Arnon TI, et al. Novel APC-like properties of human NK cells directly regulate T cell activation. J Clin Invest. 2004; 114:1612–23. [PubMed: 15578093]
14. Welner RS, Pelayo R, Garrett KP, Chen X, Perry SS, Sun XH, et al. Interferon-producing killer dendritic cells (IKDCs) arise via a unique differentiation pathway from primitive c-$kit^{Hi}CD62L^{+}$ lymphoid progenitors. Blood. 2007; 109:4825–931. [PubMed: 17317852]
15. Pletneva M, Fan H, Park JJ, Radojcic V, Jie C, Yu Y, et al. IFN-producing killer dendritic cells are antigen-presenting cells endowed with T-cell cross-priming capacity. Cancer Res. 2009; 69:6607–14. [PubMed: 19679552]
16. Himoudi N, Yan M, Bouma G, Morgenstern D, Wallace R, Seddon B, et al. Migratory and antigen presentation functions of IFN-producing killer dendritic cells. Cancer Res. 2009; 69:6598–606. [PubMed: 19654308]
17. Terme M, Mignot G, Ullrich E, Bonmort M, Minard-Colin V, Jacquet A, et al. The dendritic cell-like functions of IFN-producing killer dendritic cells reside in the $CD11b^{+}$ subset and are licensed by tumor cells. Cancer Res. 2009; 69:6590–7. [PubMed: 19679551]
18. Baxter AG. The origin and application of experimental autoimmune encephalomyelitis. Nat Rev Immunol. 2007; 7:904–12. [PubMed: 17917672]
19. Legge KL, Gregg RK, Maldonado-Lopez R, Li L, Caprio JC, Moser M, et al. On the role of dendritic cells in peripheral T cell tolerance and modulation of autoimmunity. J Exp Med. 2002; 196:217–27. [PubMed: 12119346]
20. Rynda A, Maddaloni M, Mierzejewska D, Ochoa-Repáraz J, Maslanka T, Crist K, et al. Low-dose tolerance is mediated by the microfold cell ligand, reovirus protein sigma1. J Immunol. 2008; 180:5187–200. [PubMed: 18390700]
21. Rynda A, Maddaloni M, Ochoa-Repáraz J, Callis G, Pascual DW. IL-28 supplants requirement for T_{reg} cells in protein σ1-mediated protection against murine experimental autoimmune encephalomyelitis (EAE). PLoS One. 2010; 5:e8720. [PubMed: 20090936]
22. Rynda-Apple A, Huarte E, Maddaloni M, Callis G, Skyberg JA, Pascual DW. Active immunization using a single dose immunotherapeutic abates established EAE via IL-10 and regulatory T cells. Eur J Immunol. 2011; 41:313–23. [PubMed: 21268002]
23. Fritz RB, Zhao ML. Regulation of experimental autoimmune encephalomyelitis in the C57BL/6J mouse by $NK1.1^{+}$, $DX5^{+}$, $\alpha\beta^{+}$ T cells. J Immunol. 2001; 166:4209–15. [PubMed: 11238673]
24. Zhang B, Yamamura T, Kondo T, Fujiwara M, Tabira T. Regulation of experimental autoimmune encephalomyelitis by natural killer (NK) cells. J Exp Med. 1997; 186:1677–87. [PubMed: 9362528]
25. Al-Falahi Y, Sand KL, Knudsen E, Damaj BB, Rolin J, Maghazachi AA. Splenic natural killer cell activity in two models of experimental neurodegenerative diseases. J Cell Mol Med. 2009; 13:2693–703. [PubMed: 19397784]
26. Xu W, Fazekas G, Hara H, Tabira T. Mechanism of natural killer (NK) cell regulatory role in experimental autoimmune encephalomyelitis. J Neuroimmunol. 2005; 163:24–30. [PubMed: 15885305]
27. Hao J, Liu R, Piao W, Zhou Q, Vollmer TL, Campagnolo DI, et al. Central nervous system (CNS)-resident natural killer cells suppress Th17 responses and CNS autoimmune pathology. J Exp Med. 2010; 207:1907–21. [PubMed: 20696699]
28. Huang D, Shi FD, Jung S, Pien GC, Wang J, Salazar-Mather TP, et al. The neuronal chemokine CX3CL1/fractalkine selectively recruits NK cells that modify experimental autoimmune encephalomyelitis within the central nervous system. FASEB J. 2006; 20:896–905. [PubMed: 16675847]

29. Hammarberg H, Lidman O, Lundberg C, Eltayeb SY, Gielen AW, Muhallab S, et al. Neuroprotection by encephalomyelitis: rescue of mechanically injured neurons and neurotrophin production by CNS-infiltrating T and natural killer cells. J Neurosci. 2000; 20:5283–91. [PubMed: 10884312]
30. Takahashi K, Miyake S, Kondo T, Terao K, Hatakenaka M, Hashimoto S, et al. Natural killer type 2 bias in remission of multiple sclerosis. J Clin Invest. 2001; 107:R23–9. [PubMed: 11238569]
31. Munschauer FE, Hartrich LA, Stewart CC, Jacobs L. Circulating natural killer cells but not cytotoxic T lymphocytes are reduced in patients with active relapsing multiple sclerosis and little clinical disability as compared to controls. J Neuroimmunol. 1995; 62:177–81. [PubMed: 7499506]
32. Batoulis H, Addicks K, Kuerten S. Emerging concepts in autoimmune encephalomyelitis beyond the CD4/T(H)1 paradigm. Ann Anat. 2010; 192:179–93. [PubMed: 20692821]
33. Spits H, Lanier LL. Natural killer or dendritic: what's in a name? Immunity. 2007; 26:11–6. [PubMed: 17241957]
34. Winkler-Pickett R, Young HA, Cherry JM, Diehl J, Wine J, Back T, et al. In vivo regulation of experimental autoimmune encephalomyelitis by NK cells: alteration of primary adaptive responses. J Immunol. 2008; 180:4495–506. [PubMed: 18354171]
35. Cooper MA, Fehniger TA, Turner SC, Chen KS, Ghaheri BA, Ghayur T, et al. Human natural killer cells: a unique innate immunoregulatory role for the $CD56^{bright}$ subset. Blood. 2001; 97:3146–51. [PubMed: 11342442]
36. Airas L, Saraste M, Rinta S, Elovaara I, Huang YH, Wiendl H. Immunoregulatory factors in multiple sclerosis patients during and after pregnancy: relevance of natural killer cells. Clin Exp Immunol. 2008; 151:235–43. [PubMed: 18062798]
37. Lu L, Ikizawa K, Hu D, Werneck MB, Wucherpfennig KW, Cantor H. Regulation of activated $CD4^+$ T cells by NK cells via the Qa-1-NKG2A inhibitory pathway. Immunity. 2007; 26:593–604. [PubMed: 17509909]
38. Penack O, Gentilini C, Fischer L, Asemissen AM, Scheibenbogen C, Thiel E, et al. $CD56^{dim}CD16^{neg}$ cells are responsible for natural cytotoxicity against tumor targets. Leukemia. 2005; 19:835–40. [PubMed: 15744340]
39. Greenwald RJ, Freeman GJ, Sharpe AH. The B7 family revisited. Annu Rev Immunol. 2005; 23:515–48. [PubMed: 15771580]
40. Carter LL, Leach MW, Azoitei ML, Cui J, Pelker JW, Jussif J, et al. PD-1/PD-L1, but not PD-1/PD-L2, interactions regulate the severity of experimental autoimmune encephalomyelitis. J Neuroimmunol. 2007; 182:124–34. [PubMed: 17182110]
41. Moon JJ, Chu HH, Pepper M, McSorley SJ, Jameson SC, Kedl RM, et al. Naive $CD4^+$ T cell frequency varies for different epitopes and predicts repertoire diversity and response magnitude. Immunity. 2007; 27:203–13. [PubMed: 17707129]
42. Huarte E, Sarobe P, Lu J, Casares N, Lasarte JJ, Dotor J, et al. Enhancing immunogenicity of a CTL epitope from carcinoembryonic antigen by selective amino acid replacements. Clin Cancer Res. 2002; 8:2336–44. [PubMed: 12114438]
43. Sabatino JJ Jr, Huang J, Zhu C, Evavold BD. High prevalence of low affinity peptide-MHC II tetramer-negative effectors during polyclonal $CD4^+$ T cell responses. J Exp Med. 2011; 208:81–90. [PubMed: 21220453]
44. Feng X, Yan J, Wang Y, Zierath JR, Nordenskjold M, Henter JI, et al. The proteasome inhibitor bortezomib disrupts tumor necrosis factor-related apoptosis-inducing ligand (TRAIL) expression and natural killer (NK) cell killing of TRAIL receptor-positive multiple myeloma cells. Mol Immunol. 2010; 47:2388–96. [PubMed: 20542572]
45. Murphy TL, Murphy KM. Slow down and survive: Enigmatic immunoregulation by BTLA and HVEM. Annu Rev Immunol. 2010; 28:389–411. [PubMed: 20307212]
46. Ochoa-Repáraz J, Mielcarz DW, Begum-Haque S, Kasper LH. Gut, bugs, and brain: Role of commensal bacteria in the control of central nervous system disease. Ann Neurol. 2011; 69:240–7. [PubMed: 21387369]
47. Steinman L, Zamvil SS. Virtues and pitfalls of EAE for the development of therapies for multiple sclerosis. Trends Immunol. 2005; 26:565–71. [PubMed: 16153891]

48. Fontoura P, Garren H. Multiple sclerosis therapies: molecular mechanisms and future. Results Probl Cell Differ. 2010; 51:259–85. [PubMed: 20838962]
49. Saraste M, Irjala H, Airas L. Expansion of $CD56^{Bright}$ natural killer cells in the peripheral blood of multiple sclerosis patients treated with interferon-beta. Neurol Sci. 2007; 28:121–6. [PubMed: 17603762]
50. Kastrukoff LF, Lau A, Wee R, Zecchini D, White R, Paty DW. Clinical relapses of multiple sclerosis are associated with 'novel' valleys in natural killer cell functional activity. J Neuroimmunol. 2003; 145:103–14. [PubMed: 14644036]
51. Bielekova B, Catalfamo M, Reichert-Scrivner S, Packer A, Cerna M, Waldmann TA, et al. Regulatory $CD56^{bright}$ natural killer cells mediate immunomodulatory effects of IL-2Rα-targeted therapy (daclizumab) in multiple sclerosis. Proc Natl Acad Sci U S A. 2006; 103:5941–6. [PubMed: 16585503]
52. Bielekova B, Howard T, Packer AN, Richert N, Blevins G, Ohayon J, et al. Effect of anti-CD25 antibody daclizumab in the inhibition of inflammation and stabilization of disease progression in multiple sclerosis. Arch Neurol. 2009; 66:483–9. [PubMed: 19364933]
53. Rio J, Nos C, Tintoré M, Téllez N, Galán I, Pelayo R, et al. Defining the response to interferon-β in relapsing-remitting multiple sclerosis patients. Ann Neurol. 2006; 59:344–52. [PubMed: 16437558]
54. Axtell RC, de Jong BA, Boniface K, van der Voort LF, Bhat R, De Sarno P, et al. T helper type 1 and 17 cells determine efficacy of interferon-β in multiple sclerosis and experimental encephalomyelitis. Nat Med. 2010; 16:406–12. [PubMed: 20348925]
55. Warabi Y, Matsumoto Y, Hayashi H. Interferon beta-1b exacerbates multiple sclerosis with severe optic nerve and spinal cord demyelination. J Neurol Sci. 2007; 252:57–61. [PubMed: 17125797]
56. Begum-Haque S, Christy M, Ochoa-Reparaz J, Nowak EC, Mielcarz D, Haque A, et al. Augmentation of regulatory B cell activity in experimental allergic encephalomyelitis by glatiramer acetate. J Neuroimmunol. 2011
57. Carter NJ, Keating GM. Glatiramer acetate: a review of its use in relapsing-remitting multiple sclerosis and in delaying the onset of clinically definite multiple sclerosis. Drugs. 2010; 70:1545–77. [PubMed: 20687620]
58. Hauser SL, Waubant E, Arnold DL, Vollmer T, Antel J, Fox RJ, et al. B-cell depletion with rituximab in relapsing-remitting multiple sclerosis. N Engl J Med. 2008; 358:676–88. [PubMed: 18272891]
59. Rose JW, Watt HE, White AT, Carlson NG. Treatment of multiple sclerosis with an anti-interleukin-2 receptor monoclonal antibody. Ann Neurol. 2004; 56:864–7. [PubMed: 15499632]
60. Coles A, Deans J, Compston A. Campath-1H treatment of multiple sclerosis: lessons from the bedside for the bench. Clin Neurol Neurosurg. 2004; 106:270–4. [PubMed: 15177782]
61. Perona-Wright G, Mohrs K, Szaba FM, Kummer LW, Madan R, Karp CL, et al. Systemic but not local infections elicit immunosuppressive IL-10 production by natural killer cells. Cell Host Microbe. 2009; 6:503–12. [PubMed: 20006839]
62. Cheung TC, Steinberg MW, Oborne LM, Macauley MG, Fukuyama S, Sanjo H, et al. Unconventional ligand activation of herpesvirus entry mediator signals cell survival. Proc Natl Acad Sci U S A. 2009; 106:6244–9. [PubMed: 19332782]
63. Fan Z, Yu P, Wang Y, Fu ML, Liu W, Sun Y, et al. NK-cell activation by LIGHT triggers tumor-specific $CD8^{+}$ T-cell immunity to reject established tumors. Blood. 2006; 107:1342–51. [PubMed: 16223768]
64. Gonzalez LC, Loyet KM, Calemine-Fenaux J, Chauhan V, Wranik B, Ouyang W, et al. A coreceptor interaction between the CD28 and TNF receptor family members B and T lymphocyte attenuator and herpesvirus entry mediator. Proc Natl Acad Sci U S A. 2005; 102:1116–21. [PubMed: 15647361]
65. Sakoda Y, Park JJ, Zhao Y, Kuramasu A, Geng D, Liu Y, et al. Dichotomous regulation of GVHD through bidirectional functions of the BTLA-HVEM pathway. Blood. 2011; 117:2506–14. [PubMed: 21220749]
66. Hubert P, Jacobs N, Caberg JH, Boniver J, Delvenne P. The cross-talk between dendritic and regulatory T cells: good or evil? J Leukoc Biol. 2007; 82:781–94. [PubMed: 17652446]

67. Della Chiesa M, Vitale M, Carlomagno S, Ferlazzo G, Moretta L, Moretta A. The natural killer cell-mediated killing of autologous dendritic cells is confined to a cell subset expressing CD94/NKG2A, but lacking inhibitory killer Ig-like receptors. Eur J Immunol. 2003; 33:1657–66. [PubMed: 12778484]

68. Mailloux AW, Young MR. NK-dependent increases in CCL22 secretion selectively recruits regulatory T cells to the tumor microenvironment. J Immunol. 2009; 182:2753–65. [PubMed: 19234170]

69. Schreiner B, Bailey SL, Shin T, Chen L, Miller SD. PD-1 ligands expressed on myeloid-derived APC in the CNS regulate T-cell responses in EAE. Eur J Immunol. 2008; 38:2706–17. [PubMed: 18825752]

Highlights

- IKDCs are recruited to CNS subsequent MOG-pσ1 treatment of EAE mice.
- IKDCs stimulate and recruit activated MOG-specific T_{reg} cells to the CNS.
- IKDCs are able to kill activated $CD4^+$ T cells and mature dendritic cells.
- IKDCs express elevated levels of HVEM, while CD4 T cells and B cells express LIGHT and BTLA
- Adoptive transfer of MHC-II^{high} IKDCs confers protection against EAE.

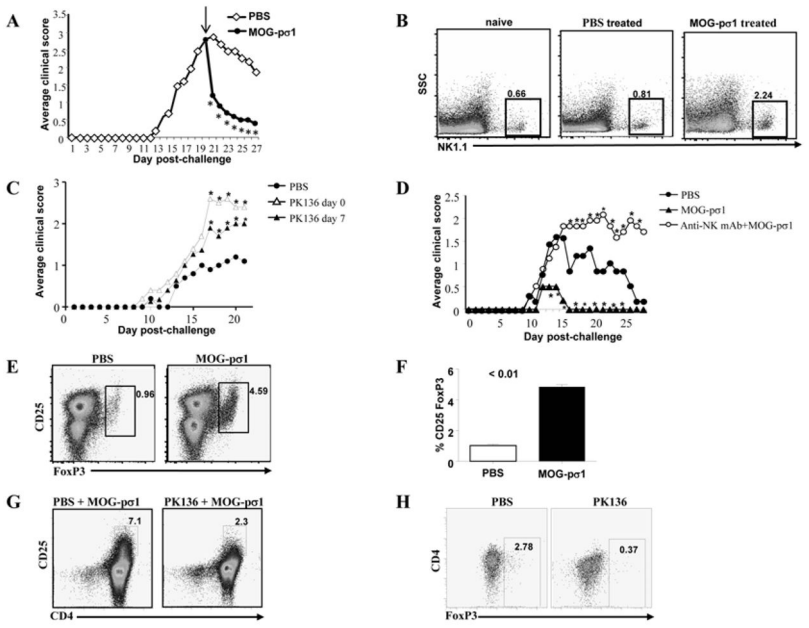

Fig. 1.

MOG-pσ1 reduces EAE by recruiting T_{reg} cells in a $NK1.1^+$ cell-dependent fashion. A. C57BL/6 mice were orally treated with 50 μg of MOG-pσ1 or with PBS 20 days after $MOG_{35–55}$-induced EAE. MOG-pσ1-treated mice showed improved resolution of clinical disease 24 h after treatment. The average score of 5 mice per group is depicted. *$P < 0.05$ versus PBS-treated group. A representative experiment of 8 is shown. B. Naïve C57BL/6 mice (left) or those induced with EAE were treated 18 days later with PBS (center) or 50 μg of MOG-pσ1 (right), and the percentage of NK1.1 cells in the spleens was evaluated 24 h later. C. C57BL/6 mice were treated weekly with PK136 depleting mAb starting at the time of EAE induction or 7 days later and monitored for disease course. D. C57BL/6 mice, either depleted or not of $NK1.1^+$ cells by PK136 mAb treatment, were then orally dosed with MOG-pσ1 or PBS at the time of EAE induction, and monitored for disease course: *$P <$ 0.05 versus PBS. E and F. EAE was induced in GFP-FoxP3 reporter mice and 18 days later orally dosed with 50 μg of MOG-pσ1 or PBS. Twenty-four hours later, mice were sacrificed, and spleens were removed and cultured for 4 days in the presence of $MOG_{35–55}$ and feeder cells before being analyzed by flow cytometry. F. The average percentage of splenic $FoxP3^+$ $CD25^+CD4^+$ T cells is shown after treatment with PBS (open bar) or MOG-pσ1 (black bar). G. LNs from C57BL/6 mice with EAE, depleted of NK1.1 cells (right panel), or not (left panel), were stained for CD4 and CD25 24 h after treatment with MOG-pσ1. The number of $CD25^+CD4^+$ T cells is shown. H. Evaluation of FoxP3 expression by CNS-infiltrating BM-derived cells from GFP-FoxP3 reporter mice with EAE treated with PBS (left panel) or PK136 mAb (right panel) is shown.

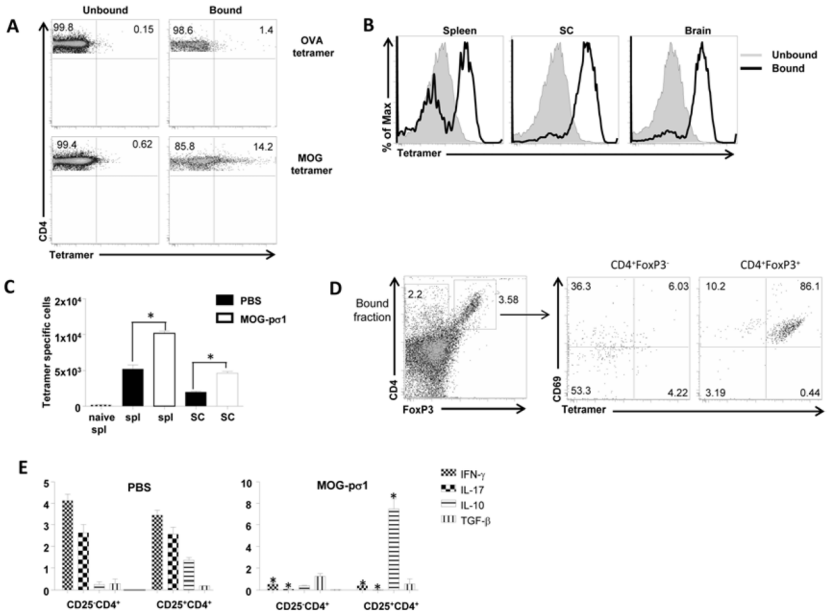

Fig. 2.

MOG-pσ1 treatment increases the number of MOG-specific T_{reg} cells. A. Splenocytes from C57BL/6 EAE mice were incubated with APC-$OVA_{329–337}$ (upper panels) or $MOG_{42–55}$ tetramer (lower panels) and then reacted with magnetic anti-APC-beads. Magnetically bound (right panels) and unbound cell fractions (left panels) were then stained for CD4, CD11b, and CD45. A representative experiment of 3 is shown. B. Spleens and CNS-infiltrating lymphocytes from GFP-FoxP3 reporter mice were isolated, stained with APC-MOG tetramer, and again divided into bound and unbound cell fractions. Histograms representing tetramer staining for both fractions are shown. C. Absolute number of MOG-specific T_{reg} cells in the bound fraction of indicated groups is shown. *$P < 0.05$ versus PBS-treated mice. D. SC-infiltrating lymphocytes were purified from GFP-FoxP3 EAE mice and separated into MOG-tetramer bound and unbound fractions. Cells were then stained for CD4, CD11b, CD45, and CD69, and the percentage of $CD69^+$ tetramer-specific cells is shown for $FoxP3^+CD4^+$ and $FoxP3^-CD4^+$ T cells in the bound fraction. E. $CD25^+CD4^+$ and $CD25^-CD4^+$ T cells were purified from PBS- or MOG-pσ1-treated mice 15 days after EAE induction, and were restimulated in vitro with $MOG_{35–55}$ in the presence of irradiated APCs. Cytokine levels (mean ∀ SEM from triplicate cultures) in culture supernatants were measured by cytokine-specific ELISAs 4 days after culture, and values are corrected for cytokine levels produced by unstimulated cells. *$P < 0.05$ versus PBS-treated mice.

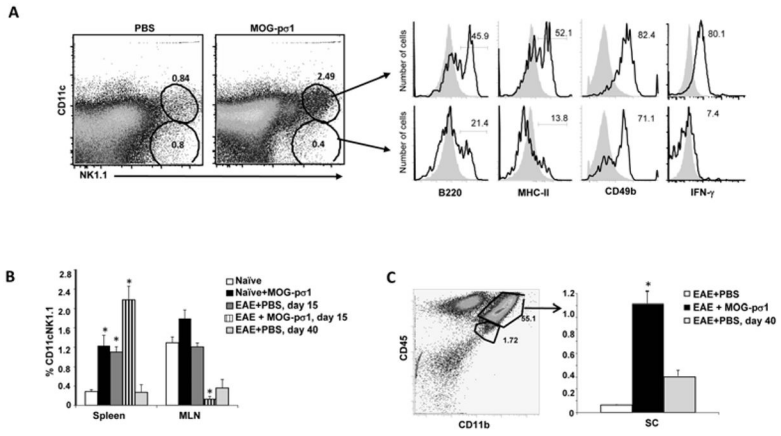

Fig. 3.

MOG-pσ1 increases the infiltration of $CD11c^{+}NK1.1^{+}$ IKDCs. A. Lymphocytes from PBS- or MOG-pσ1-treated EAE mice were isolated, restimulated with $MOG_{35–55}$, and stained for expression of NK1.1, CD11c, MHC class II, B220, CD49b, and intracellular IFN-γ. *P < 0.05 versus PBS-treated mice. A representative experiment of three is depicted. B. Percentages of $CD11c^{+}NK1.1^{+}$ cells in spleens and MLNs of PBS- or MOG-pσ1-treated PBS-treated or EAE mice (3–5/group) are shown. Mice recovering from EAE (day 40) are also included. C. PBS- or MOG-pσ1-treated mice, as well as recovering mice (day 40 p.ch), and $CD45^{Hi}$ $CD11b^{+}$ BM-derived cells were evaluated for percentage of $CD11c^{+}NK1.1^{+}$ cells infiltrating the spinal cord (SC). *P < 0.05 versus PBS-treated mice. A representative experiment of three is depicted.

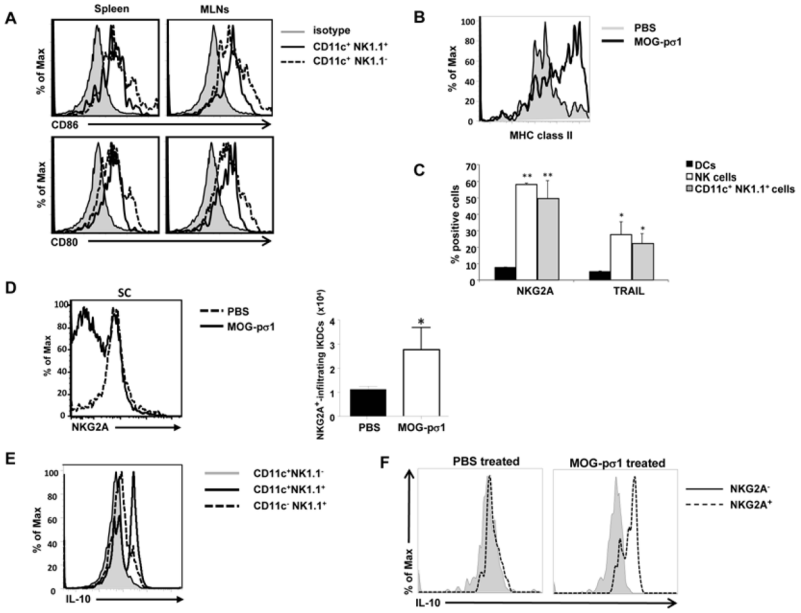

Fig. 4.

$CD11c^+NK1.1^+$ cells are phenotypically IKDCs, and the level of NKG2A decreases after MOG-pσ1 treatment. C57BL/6 mice were treated with MOG-pσ1 or PBS 20 days after induction of EAE, and 24 h later lymphocytes from spinal cord (SC), spleens, and LNs were purified and stained for analysis by flow cytometry. A. CD80 and CD86 staining was shown for DCs and $CD11c^+NK1.1^+$ cells in spleens (left panels) and MLNs (right panels); staining with an isotype control mAb is also shown (filled histogram). B. Levels of expression of MHC class II by SC-infiltrating $CD11c^+NK1.1^+$ cells are shown for PBS- and MOG-pσ1-treated mice. C. Percentages of $NKG2A^+$ and $TRAIL^+$ NK cells, DCs, and $CD11c^+NK1.1^+$ cells obtained from spleens of EAE mice are shown. $^*P < 0.05$, $^{**}P < 0.010$ versus DCs. D. NKG2A expression is reduced in SC-infiltrating $NK1.1^+$ cells following MOG-pσ1 treatment (data depicted are representative of 5 mice/group), but absolute number of CNS-infiltrating $NKG2A^+$ IKDCs is overall enhanced. $^*P < 0.05$ versus PBS-treated mice. E. At the peak of disease, intracellular IL-10 staining was analyzed for $CD11c^+NK1.1^-$, $CD11c^+NK1.1^+$, and $CD11c^-NK1.1^+$ subsets. F. IL-10 is predominantly produced by $NKG2A^+$ IKDC subset induced by MOG-pσ1 treatment. Data are of 3 mice/group.

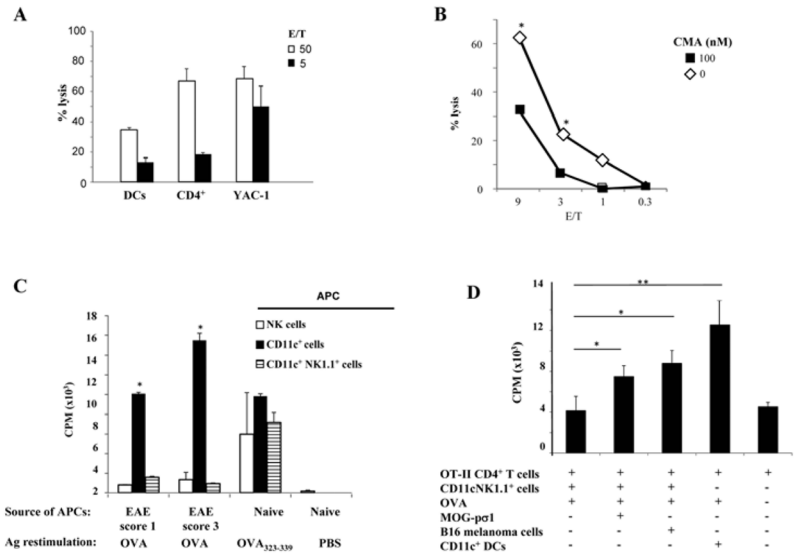

Fig. 5.

$CD11c^+NK1.1^+$ cells are functionally IKDCs and able to kill $CD4^+$ T cells and DCs and stimulate the proliferation of OT-II cells. A. Splenic and LN $CD11c^+NK1.1^+$ cells from EAE mice were cell-sorted and cultured for 3 days in the presence of IL-2 before performing a ^{51}Cr release assay against autologous CD3/CD28 activated $CD4^+$ T cells, bone marrow-derived DCs, or YAC-1 cells at the indicated effector: target (E/T) ratios. B. ^{51}Cr release assay using $CD11c^+NK1.1^+$ effector cells against YAC-1 target cells in the presence of concanamycin A (CMA) or control media was performed at various E/T ratios. $^*P \leq 0.05$ versus CMA. C. DCs and NK cells, as well as $CD11c^+NK1.1^+$ cells, were cell-sorted from splenocytes obtained from C57BL/6 mice 10 or 20 days (clinical scores 1 and 3, respectively) after EAE induction and co-cultured with OT-II $CD4^+$ T cells and OVA protein. As positive control, NK cells, DCs, and $CD11c^+NK1.1^+$ cells from naive mice were pulsed with $OVA_{323–339}$ and compared to cultures stimulated in the absence of Ag. The mean of triplicate cultures ∀ SD is depicted and is representative from three experiments; $^*P < 0.05$ depicts significant differences for OVA presentation by $CD11c^+$ DCs versus $CD11c^+NK1.1^+$ cells. D. $CD11c^+NK1.1^+$ cells and DCs were cell-sorted from C57BL/6 mice at the peak of the disease and preincubated or not with B16F1 melanoma cells or MOG-pσ1 plus OVA protein before the co-culture with purified OT-II CD^+ T cells. The mean of triplicate cultures ∀ SD representative of two experiments is shown; $^*P < 0.05$, $^{**}P < 0.010$ versus OVA-pulsed $CD11c^+NK1.1^+$ cells.

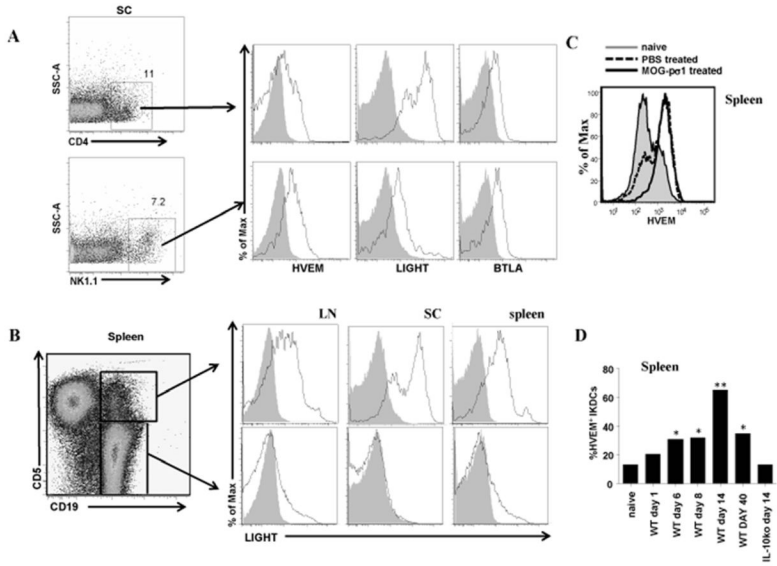

Fig. 6.

MOG-pσ1 treatment induces an up-regulation of HVEM in NK1.1$^+$ cells. A. C57BL/6 mice were treated with MOG-pσ1 or PBS 20 days after EAE induction, and 24 h after treatment, spleens and SC cells were stained for CD4, NK1.1, HVEM, LIGHT, and BTLA. Percentages of infiltrating CD4$^+$ T cells and IKDCs in the SC of PBS- or MOG-pσ1-treated mice are shown. Staining by an isotype control mAb is shown as filled histogram; * $P \leq 05$. A representative experiment of three is depicted. B. EAE was induced in C57BL/6 mice, and 20 days later, splenic, LN, and SC lymphocytes were purified and analyzed by flow cytometry for CD5, CD19, HVEM, LIGHT, and BTLA expression. Gating strategy is shown on the left-hand side. Histograms and percentages of positive cells are shown on at the right-hand side. Staining by an isotype control mAb is shown as filled histogram. A representative mouse out of five is shown. C. A histogram depicts HVEM levels for splenic NK1.1$^+$ cells from naïve and PBS- or MOG-pσ1-treated EAE mice. A representative experiment of three is shown. D. Percentages of splenic CD11c$^+$NK1.1$^+$ IKDCs expressing HVEM at different time points after EAE induction are shown. Percentages of HVEM$^+$ IKDCs from IL-10$^{-/-}$ mice at day 14 after EAE induction are also shown. *$P < 0.05$, **$P \leq 0.01$ versus naive mice.

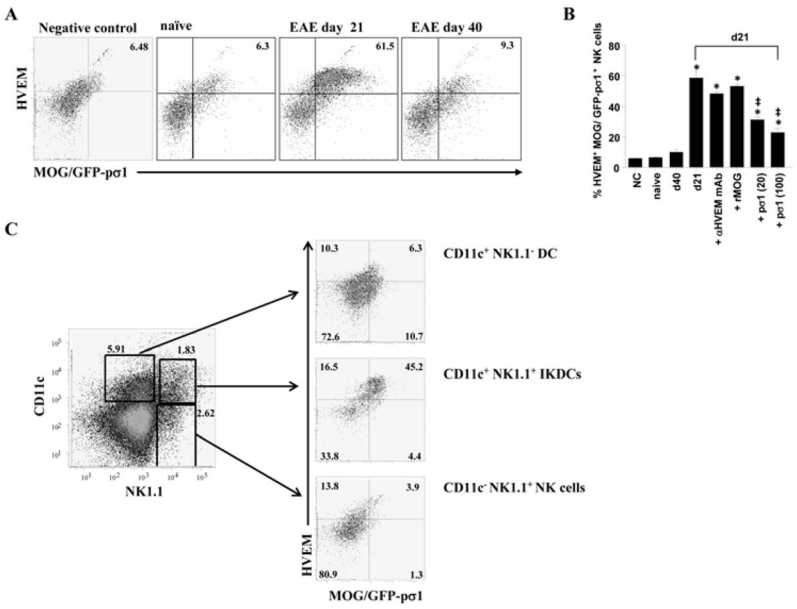

Fig. 7.

HVEM$^+$ IKDCs bind MOG-pσ1. A. Splenic and LN lymphocytes from naïve- or EAE-challenged mice 10 or 40 days earlier were tested for their ability to bind MOG/GFP-pσ1 following 4 days restimulation with $MOG_{35–55}$ and IL-2. Negative control cells were stained with MOG-pσ1 instead of MOG/GFP-pσ1. Data depict cells gated on NK1.1$^+$ cells (representative of four mice/group). B. Percentages of NK1.1 HVEM$^+$ cells binding to MOG/GFP-pσ1 were assessed. Anti- HVEM mAb (20 μg/ml), recombinant MOG (20 μg/ml), or recombinant pσ1 (20 and 100 μg/ml) was added when indicated. Each column represents the mean ± SD from 4 mice/group. $^{**}P \leq 0.01$ versus negative control (NC); $^{‡}P < 0.01$ versus d21 MOG/GPF-pσ1 staining. (C) Splenocytes from a mouse (representative of 3 mice) at the peak of the disease were gated on CD11c$^+$ DCs, CD11c$^+$NK1.1$^+$ cells (IKDCs), and NK1.1$^+$ CD11c$^-$ NK cells and analyzed for MOG/GFP-pσ1 binding and HVEM expression.

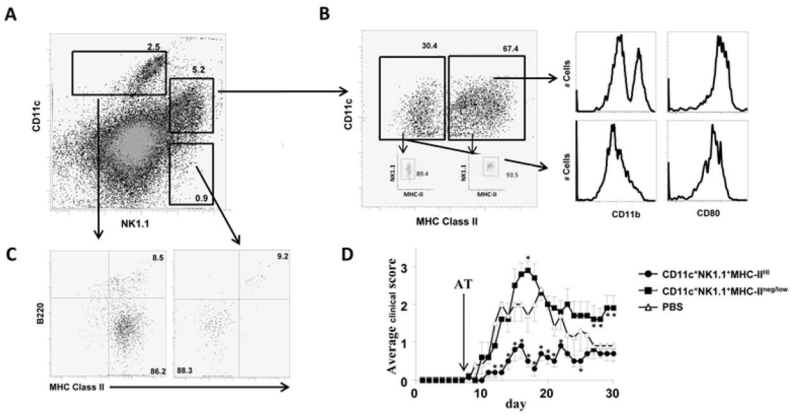

Fig. 8.

Adoptive transfer of IKDCs protects against EAE. A. C57BL/6 mice were challenged with MOG and 15 days later treated with 50 μg of MOG-pσ1. Twenty-four hours later, mice were sacrificed, and their spleens and LNs were combined and stained with CD11c, NK1.1, MHC class II, and B220. $CD11c^{+}NK1.1^{+}$ cells were sorted based on their MHC class II expression. B. MHC class II^{Hi}- and MHC class II^{low}-sorted cells were analyzed for CD11b and CD80 expression. The purity of the sorting is shown on the inserted panels. C. $CD11c^{+}$ DC and $NK1.1^{+}$ cells were analyzed for B220 and MHC-class II expression. As expected, only $CD11c^{+}$ cells expressed high levels of MHC class II. D. 1×10^{5} $CD11c^{+}NK1.1^{+}$MHC class II^{hi} cells (activated IKDCs) or $CD11c^{+}NK1.1^{+}$MHC class II^{low} (unactivated) cells were adoptively transferred (AT) into C57BL/6 mice previously induced with EAE 7 days earlier and monitored for disease course. Average score of five mice is shown. $*P < 0.05$, $**P < 0.010$ versus PBS.

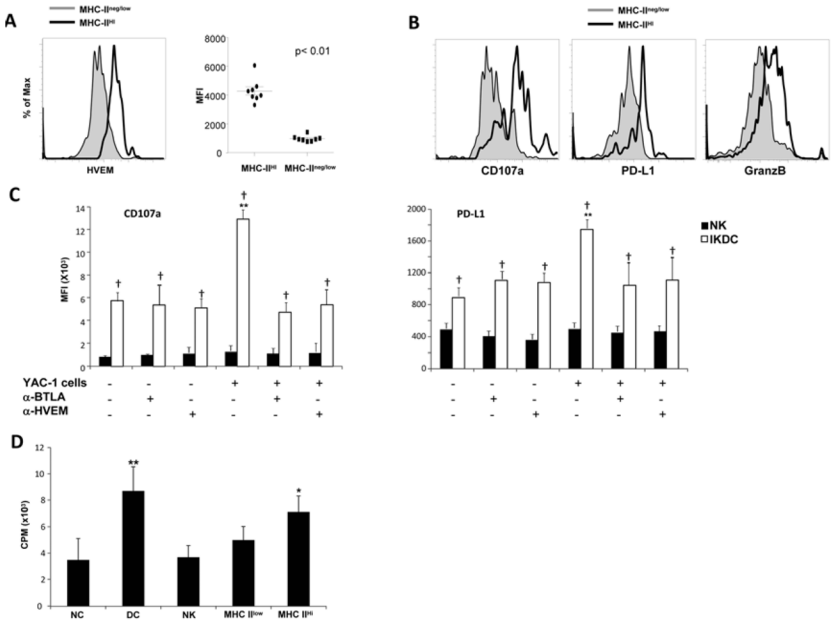

Fig. 9.

Activated IKDCs, but not NK cells, up-regulate HVEM, CD107a, and PDL-1. A. C57BL/6 mice were challenged with MOG, and 15 days later their splenocytes were analyzed for HVEM expression. Only $CD11c^{+}NK1.1^{+}$MHC class II^{Hi} IKDCs, but not $CD11c^{+}NK1.1^{+}$MHC class $^{intermediate/low}$ cells, up-regulated HVEM expression. Left panel shows a representative histogram. Right panel shows the individual MFI values and the mean for 8 mice/group. B and C. IKDCs and NK cells were cultured in the presence or absence of YAC-1 cells and anti-BTLA and anti-HVEM mAbs, and CD107a, PD-L1, and granzyme B expression were measured by flow cytometry. YAC-1 cell co-culture increases CD107a degranulation and PD-L1 overexpression by IKDCs, and anti-BTLA or anti-HVEM mAb treatment blocks such up-regulation. $^{**}P \leq 0.01$ versus PBS-treated mice; $^{\dagger}P < 0.01$ versus NK cells. D. $NK1.1^{+}$ $CD11c^{-}$, $NK1.1^{-}$ $CD11c^{+}$, $NK1.1^{+}$ $CD11c^{+}$ MHC class II^{Hi}, and $NK1.1^{+}$ $CD11c^{+}$ MHC class $II^{intermediate/low}$ cells (2×10^{4}) were pulsed with OVA overnight and then co-cultured with 1×10^{5} OT-II $CD4^{+}$ T cells, and ^{3}H-thymidine incorporation was measured after 3 days of culture. $^{*}P < 0.05$, $^{**}P \leq 0.01$ versus negative control (NC) group (without Ag-presenting cells).